Society For Biomaterials

Development of a chemically extracted acellular muscle scaffold seeded with amniotic epithelial cells to promote spinal cord repair

Hui Xue,[1*] Xiu-Ying Zhang,[1,2*] Jia-Mei Liu,[1] Yu Song,[1,3] Yi-Fan Li,[4] Dong Chen[5]

[1]Department of Histology & Embryology, Bethune School of Medical Science, Jilin University, Changchun 130021, People's Republic of China
[2]Department of Fundamental Nursing, School of Nursing, Jilin University, Changchun 130021, People's Republic of China
[3]Department of Anatomy, Changchun Medical College, Changchun 130021, People's Republic of China
[4]Department of Anatomy, Changchun University of Chinese Medicine, Changchun 130021, People's Republic of China
[5]Department of Histology & Embryology, Guangdong Medical College, Dongguan 523808, People's Republic of China

Received 21 November 2011; revised 26 April 2012; accepted 1 June 2012
Published online 25 July 2012 in Wiley Online Library (wileyonlinelibrary.com). DOI: 10.1002/jbm.a.34311

Abstract: Bridging strategies are essential for spinal cord repair in order to provide a physical substrate allowing axons to grow across the site of spinal cord lesions. In this study, we have evaluated the therapeutic effects of adding amniotic epithelial cells to a unidirectionally oriented acellular muscle scaffold and have compared this with the effect of a scaffold alone. Chemically extracted acellular muscles, with or without amniotic epithelial cells, were implanted into the lateral hemisected adult rat thoracic spinal cord. Control rats were similarly injured. After 4 weeks, the acellular muscle scaffolds were found to be well integrated with the host tissue. The chemically extracted acellular muscle scaffold seeded with amniotic epithelial cells promoted axonal growth in a distinctly organized and linear fashion, induced sprouting of calcitonin gene-related peptide positive axons, and was not associated with an astrocyte response. Compared with acellular muscle scaffolds alone, the addition of amniotic epithelial cells further promoted the remyelination of nerve fibers, sprouting of 5-hydroxytryptamine nerve fibers, relays of cortical motor-evoked potential and cortical somatosensory-evoked potential, and functional recovery. All these data together suggest that co-implantation of chemically extracted acellular muscle with amniotic epithelial cells may constitute a valuable approach to study and/or develop therapies for spinal cord injury. © 2012 Wiley Periodicals, Inc. J Biomed Mater Res Part A: 101A: 145–156, 2013.

Key Words: acellular scaffold, amniotic epithelial cell, spinal cord injury, nerve tissue engineering

How to cite this article: Xue H, Zhang X-Y, Liu J-M, Song Y, Li Y-F, Chen D. 2013. Development of a chemically extracted acellular muscle scaffold seeded with amniotic epithelial cells to promote spinal cord repair. J Biomed Mater Res Part A 2013:101A:145–156.

INTRODUCTION

The mammalian spinal cord was previously believed to be unable to regenerate after injury. This limited regenerative capacity of the adult spinal cord has been attributed to a host of inhibitory signals associated with the extracellular environment and with the generally low intrinsic potential of mature central nervous system neurons to regenerate.[1] By addressing each of these intrinsic or extrinsic factors individually, significant progress has been made in promoting the growth of injured adult axons.[2] These approaches include the provision of supportive substrates,[3,4] providing neurotrophic factors to injured axons,[5,6] and neutralizing inhibitory proteins at the site of injury.[7,8] Within these approaches, tissue engineering scaffolds are essential to provide a physical substrate allowing axons to grow across the lesion site, because cavity formation and glial scars are important obstacles impeding regeneration after spinal cord injury (SCI).

Extracellular matrix is the gold standard for tissue regeneration. In recent years, various synthetic and naturally derived materials, which aim to mimic native extracellular matrix, have been used to construct spinal cord scaffolds and have provided promising results toward improving the function of injured nervous tissue.[9–11] Nevertheless, because these approaches have not provided the ultimate nerve regeneration scaffold, it has been postulated that further improvements are needed for all these reported tissue engineering scaffolds in order to achieve a greater resemblance to extracellular matrix. Such approaches have included providing stimulatory cues[12] and optimization of

Additional Supporting Information may be found in the online version of this article.
*These authors contributed equally to this work.
Correspondence to: D. Chen; e-mail: nbumschendong@yahoo.com.cn or J.-M. Liu; e-mail: liujiamei100@yahoo.com.cn
Contract grant sponsor: Chinese National Natural Science Foundation; contract grant number: 30970739 (to D.C.)
Contract grant sponsor: Jilin Province Science Foundation; contract grant number: 20090726 (to J.-M.L)

scaffold internal architecture design.[13] In contrast, acellular scaffolds that directly bring the extracellular matrix of the tissue or organ into the scaffold can effectively retain the structural and functional proteins of extracellular matrix and their original three-dimensional (3D) distribution. Previously, we tried to use acellular muscle as the bridging scaffold for SCI and found that chemically extracted acellular muscle grafts provided useful biomatrices to enhance axonal sprouting and guide the sprouting axons in a distinctly organized and linear fashion in the injured spinal cord.[14] This method may help to guide sprouting axons into the spinal cord distal to the lesion site and ultimately result in effective reconnection of damaged axons with their target neurons.

Cell transplantation has been employed as another strategy to treat SCI. A wide range of cell types has been studied, such as fibroblasts, astrocytes, Schwann cells, olfactory ensheathing cells, bone marrow stromal cells, and amniotic epithelial cells (AECs).[15–17] Of these, the AEC has considerable advantageous characteristics that make it an attractive material in the field of regenerative medicine.[18] It has low immunogenicity,[19,20] has anti-inflammatory properties,[21] and can be isolated without the sacrifice of human embryos. Like embryonic stem cells, AECs retain stem cell characteristics[22] and have the potential to protect and replace damaged neural cells, but with a lower risk of tumorigenesis.[23] In addition, human AECs produce some neurotrophins such as brain-derived neurotrophic factor (BDNF) and neurotrophin (NT)-3.[24] Previous work from our laboratory demonstrates that AECs can promote neural differentiation of neural stem cells and neurite growth *in vitro*.[25] All these characteristics make the AEC a potential candidate for cell transplantation in the treatment of SCI. However, there are only few studies supporting this fact. In the present investigation, we seeded AECs into the acellular muscle bridge across the hemisected rat spinal cord. Our goal was to fabricate an engineering scaffold with ideal regeneration potential for SCI.

MATERIALS AND METHODS

Animals

Male Wistar rats (280–350 g) were purchased from the experimental animal center of Jilin University. Animals were housed in a standard cage and kept under standard laboratory conditions with the temperature at 22 ± 2°C and a 12–12 h light/dark cycle. Animal experiments related to this study were approved by the Local Ethics Committee for Animal Research at Jilin University and performed in accordance with international standards for animal welfare. All surgical procedures were performed under general anesthesia by intraperitoneal injection with 10% chloral hydrate.

Preparation of acellular muscle grafts

Adult Wistar rats were sacrificed by intraperitoneal overdose with 60 mg/kg of chloral hydrate. The bundles of paravertebral muscles were excised and longitudinally harvested. The preparation of the chemically extracted acellular muscle was based on the procedures described in a previous publication.[26] Briefly, the muscle segments were treated with a series of detergent baths consisting of sodium dodecyl sulfate (SDS; Sigma) and Triton X-100 (Sigma). All steps were performed under constant stirring at 37°C. Following this, all samples were then sterilized using 50 mg/mL of ampicillin and stored in phosphate buffered saline (PBS) at 4°C until use.

After processing, cryostat sections of the acellular muscle scaffolds were stained with hematoxylin and eosin (H&E) and examined by light microscopy.

Moisture content of the acellular muscles

Six acellular muscle scaffolds were randomly chosen for the measurement of the moisture content (MC). After removing peripheral water by blotting, the wet weights (WW) of the scaffolds were measured in Eppendorf tubes. Then, the scaffolds in Eppendorf tubes were completely dried at 37°C for 24 h, and the dry weights (DW) of the scaffolds were measured. The moisture content was calculated with the following equation: $MC = (WW - DW)/WW \times 100\%$.

Pore size of the acellular muscles

The average pore size of the scaffold was measured with Image-Pro Plus 6. Five acellular muscle scaffolds were randomly chosen. Two randomly chosen H&E-stained sections from each scaffold were photographed under the microscope. The diameters of 12 channels in each section were measured with Image-Pro Plus 6. The mean value of diameters was calculated.

AEC isolation and culture

Rat AECs were isolated from pregnant Wistar rats at gestational days 16–17 by the methods described before[25] with minor modification. In brief, uteri were excised, and the rat amnion was mechanically peeled from the embryonic rats. Then, the amniotic membranes were rinsed three times in ice-cold Hanks' solution and dissected into small pieces. After that, they were digested in Hanks' solution containing 0.125% trypsin for 7 min at room temperature. The digested AECs were collected by centrifugation at 800 rpm for 5 minutes and then cultured in Dulbecco's Modified Eagle Medium supplemented with 10% fetal calf serum, in humidified atmosphere containing 5% CO_2 at 37°C. The medium was changed every 2 days, and the cells were confluent after 3 to 4 days.

Cell labeling and seeding

When AECs were grown to 80% confluence, they were labeled by the Hoechst 33342 (5 m*M*; Sigma). After labeling, the AECs were washed three times with PBS. They were then trypsinized and resuspended in Dulbecco's Modified Eagle Medium with 10% fetal calf serum at a density of 2×10^6 viable cells/mL. The acellular muscle scaffold was trimmed to proper size and 200 μL of the cell suspension was introduced into multiple points of the scaffold with a sample microinjector (Dingguo, Beijing, China).The cell-seeded scaffolds were put into an Eppendorf tube in a humidified atmosphere with 5% CO_2 at 37°C until use.

Spinal cord hemisection and transplantation procedures

A total of 24 male Wistar rats were used in this study. They were assigned to four groups (n = 6/each): acellular muscle group; amnion epithelial cell-seeded acellular muscle group; lesion only group; and a sham operation group. The rats were anesthetized with 10% chloral hydrate solution (3.5 mL/kg). A laminectomy was performed to expose the thoracic spinal cord at T10. Iridectomy scissors were used to make a right sided hemisection of the T10 thoracic spinal cord segment, followed by the removal of a 2-mm block of the right-sided spinal cord tissue. A fine surgical blade was used to repeatedly scrape along the ventral surface of the vertebral canal in the lesional area to ensure that all lateral spinal tissue had been severed. In the treatment groups, an AEC-seeded or control medium-injected acellular muscle graft was carefully implanted into the cavity with its longitudinal axis parallel to that of the spinal cord. A piece of silicone sheeting was placed over the scaffold and dorsal surface of the cord to stabilize the scaffold within the spinal cord. In the lesion control group, the lesional cavity was left empty. The muscles and skin were then sutured layer by layer in all the animals. The rats in the sham operation group received only the laminectomy. All rats were given extensive postoperative care including daily subcutaneous ampicillin (100 mg/kg) and gentamicin (12 mg/kg) for a period of 1 week.

Behavioral testing

The hind limb locomotor function was analyzed using the Basso, Beattie, and Bresnahan (BBB) open-field locomotor test[27] at days 3, 7, 14, 21, and 28 after surgery. Because the hind limb locomotor function on the left (unaffected side) recovered quickly for the most rats (16 of 24 rats), only the right (affected side) hind limb was ranked by two blinded observers.

Electrophysiological analysis

At the end of the experiment, evoked potentials were recorded to assess functional status of motor and sensory axonal conduction based on the method described before. Basically, following general anesthesia, the rats were placed into a stereotaxic frame. After exposure of the cerebral cortex and the sciatic nerve in the right (affected side) hind limb, electrodes from a BL-410E Data Acquisition Analysis System for Life Science (Taimeng, Chengdou, China) were connected to the sciatic nerve and cerebral cortex. The latency and amplitude of cortical motor-evoked potential (CMEP) and cortical somatosensory-evoked potentials (CSEP) were detected and recorded.

Tissue processing

After the electrophysiological analysis, all rats were deeply anesthetized and intracardially perfused with 4% paraformaldehyde in PBS. The portion of the spinal cord containing the injury and adjacent portions were removed and post-fixed overnight in the same fixative. Then, the sample was soaked overnight in 15% sucrose, followed by 30% sucrose, and cut into 16-μm thick coronal sections using a cryostat. All sections were stored at −20°C until further use.

Immunofluorescence

The sections were treated with PBS containing 0.1% Triton X-100 for 30 min. Nonspecific antibody binding was blocked with 10% normal goat serum in PBS plus 5% bovine serum albumin in PBS for 1 h. Primary antibodies including neurofilament (NF, a rabbit polyclonal antibody specific for neurofilament in the neuronal axons; 1:400; Millipore), calcitonin gene-related peptide (CGRP, a rabbit polyclonal antibody; 1:2000; Milipore), 5-hydroxytryptamine (5-HT, a rabbit polyclonal antibody; 1:100; Sigma), glial fibrillary acidic protein (GFAP, a mouse monoclonal antibody specific for astrocytes; 1:100; Labvision), and myelin basic protein (MBP, a mouse monoclonal antibody specific for the myelin membrane in the central nervous system; 1:100; Chemicon) were applied for 12 h at 4°C. Fluorescein isothiocyanate (FITC)-conjugated Goat anti-rabbit (1:200; Jackson Immunoresearch Labs) or Cy3-conjugated goat anti-mouse (1:400; Jackson Immunoresearch Labs) secondary antibodies were used to visualize primary antibody binding. For negative controls, the primary antibody was replaced by PBS. After staining, the sections were observed under a fluorescence microscope using standard fluorescent filters.

Quantification of axonal regeneration, myelinated axons, and astrocytes

The method for quantification of astrocytes in spinal cord sections was developed from protocols described before.[28,29] In the lesion group, the area in tissue adjacent to the central cavity was selected; in the treated groups, the area in tissue adjacent to but not including the graft area was selected. Positive cells were quantified by identifying GFAP-positive area with Image-Pro Plus, v. 6.0. All positive areas in six microscopic high-power fields (400×) for each section were averaged. Five sections of each spinal cord at every 112 μm interval were separately analyzed and averaged. The mean value from the combined data of all six animals in each group was calculated.

Quantification of NF-positive axons, CGRP-positive axons, and MBP-positive myelin sheaths within the graft was performed using methods described elsewhere.[12,30] Briefly, three sections were randomly selected from each animal. The total number of axons or myelin sheaths penetrating the scaffold was quantified at six microscopic fields within each section at a 400× magnification. These quantified fields were distributed within three regions of each scaffold: the rostral region (0.2–0.4 mm from rostral host–implant interface), middle region (between 0.6 mm from rostral and 0.6 mm from caudal host–implant interface), and caudal region (0.2 to 0.4 mm from caudal host–implant interface). The mean number of axons or myelin sheaths obtained from three sections of each animal was defined as the number of axons or myelins. The number of axons or myelin sheaths of six animals in each group was calculated.

Statistical analysis

All values are expressed as mean ± SD. Data from BBB score, electrophysiology, and histological results were analyzed for statistical differences between multiple groups using one-way analysis of variance (ANOVA) and between two groups using Student's *t*-test. If there was a significant difference in the multiple groups, each of the two groups

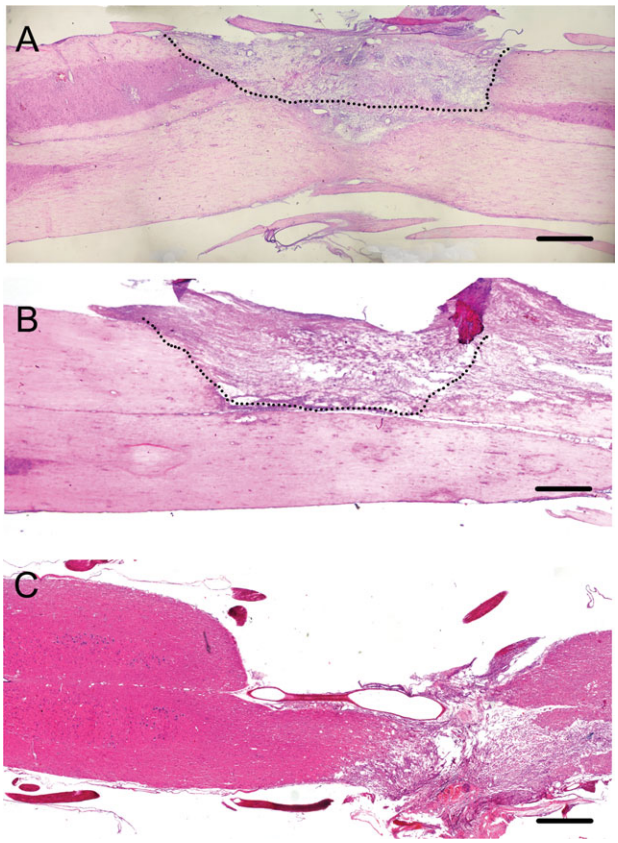

FIGURE 1. Hematoxylin/eosin (H&E) staining of coronal sections from each group. Images of representative sections from the chemically extracted acellular muscle treated group (A) and the AEC-acellular muscle treated group (B). The figures show that the scaffolds form tissue bridges between the stumps of hemisected spinal cord. The scaffolds are infiltrated by numerous host cells and integrate well with the host spinal cord. There are no fibrous scar at the interface between the scaffold and spinal cord. The broken lines mark the borders between the host spinal cords and grafts. C: Image of a section from the lesion control group. Scale bars: 500 μm. [Color figure can be viewed in the online issue, which is available at wileyonlinelibrary.com.]

was further analyzed by Student's *t*-test. A p value of <0.05 was considered statistically significant.

RESULTS

Characteristics of acellular muscle scaffold

After chemical extraction, the acellular muscle scaffolds appeared semitransparent, milkiness in color, and displayed soft properties [Supporting Information Fig. 1(A)]. In the chemically extracted acellular muscle scaffolds, all cell components were completely removed, leaving uniaxial linear channels arranged in a parallel pattern [Supporting Information Fig. 1(B)]. The moisture content of the scaffolds was 91.4 ± 6.8%. The average diameter of pores in the scaffolds was 117.3 ± 42.7 μm.

Purity of the rat AECs

After 2 h in culture, rat AECs began to attach to the bottom of the culture flask. Adherent AECs were in polygonal shape and showed several processes. To confirm the purity of the rat AECs, the CK19 immune staining was performed. The results showed that the most cells (96.7 ± 2.3%) were CK19 positive (Supporting Information Fig. 2).

Improvement of tissue repair and local environment

Four weeks after surgery, in the acellular muscle and AECs-acellular muscle treated groups, H&E staining showed that the scaffold had integrated well with the spinal cord and formed a tissue bridge between the rostral and caudal stumps of the spinal cord (Fig. 1). H&E staining results also showed substantial host cell infiltration into both kinds of scaffold. There was no difference in the cell density between the two scaffolds. No scar tissue was found at the interface between the scaffolds and spinal cord. In contrast, for the lesion control group, there was a large cavity in the spinal cord (Fig. 1). Hoechst 33342-labeled AECs were still present in the scaffolds 4 weeks after transplantation (Fig. 2).

Nerve fiber sprouting and remyelination

The effect of scaffolds on neural fiber sprouting following SCI was evaluated by NF staining analysis. NF immunohistochemical

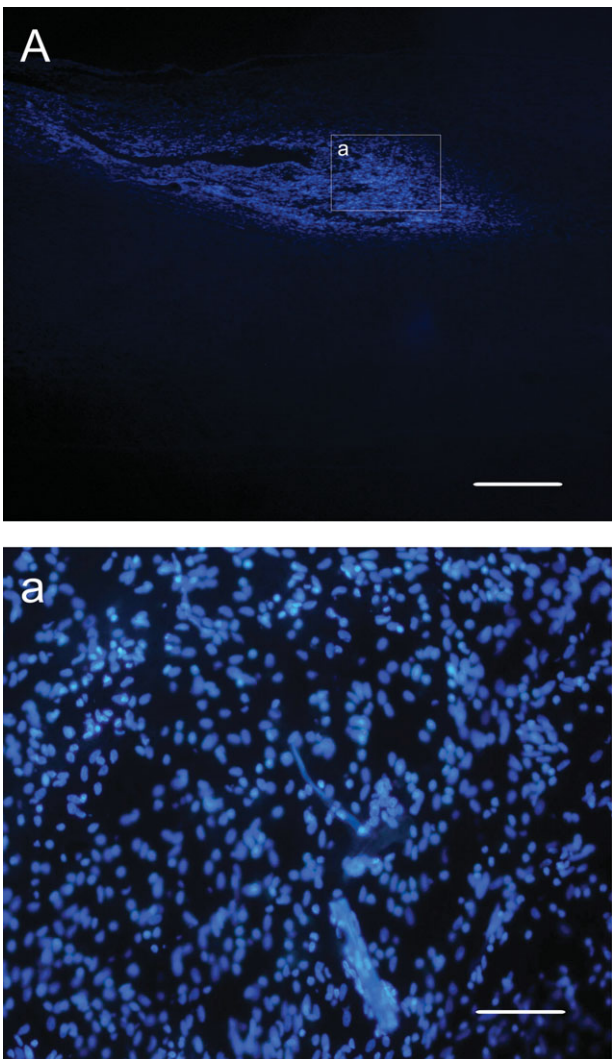

FIGURE 2. Hoechst 33342 labeled cells within the scaffold 4 weeks after transplantation. Scale bars: A, 500 μm; a, 100 μm. [Color figure can be viewed in the online issue, which is available at wileyonlinelibrary.com.]

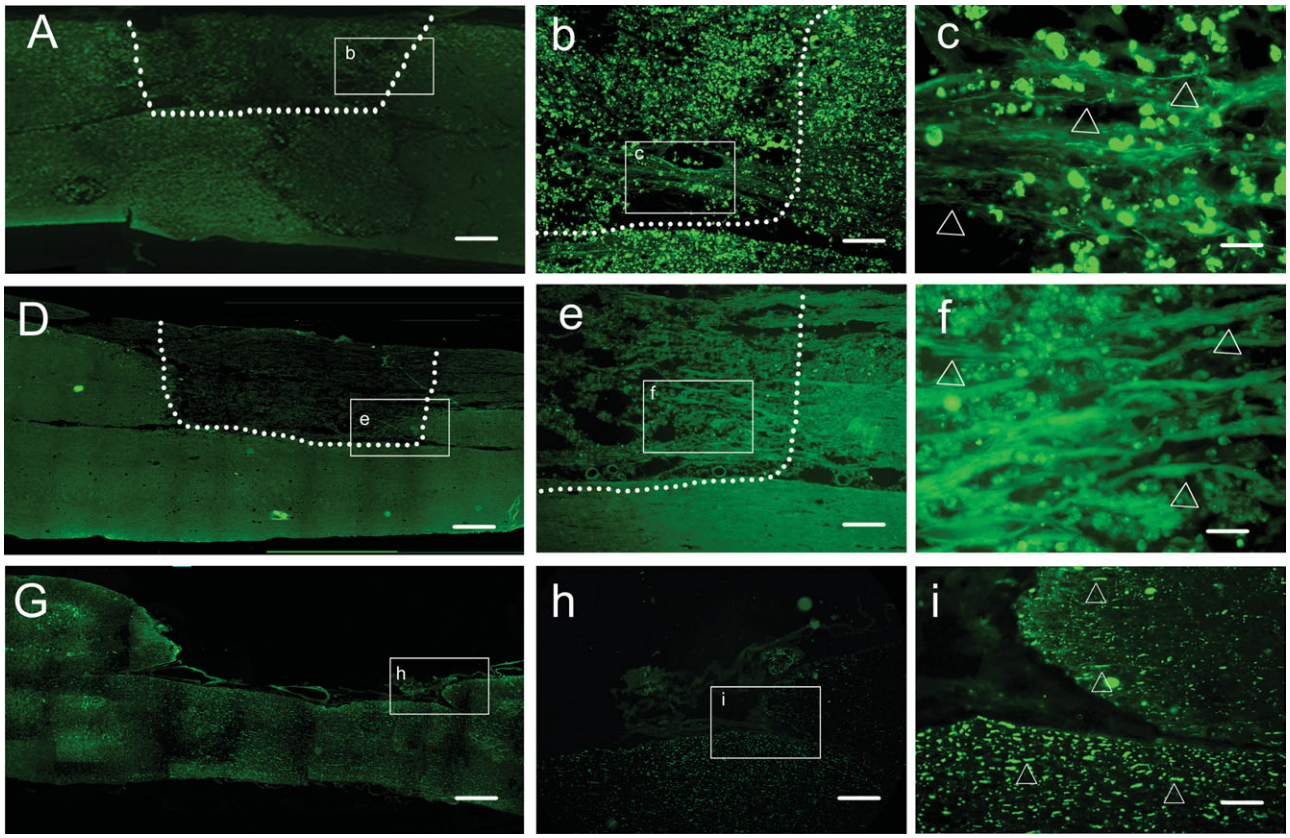

FIGURE 3. Sprouting axons 28 days after surgery, NF immunofluorescent staining. A, b, and c: chemically extracted acellular muscle; D, e, and f: AEC-acellular muscle; G, h, and i: lesion only. Note that the sprouting axons within the two types of scaffolds are distributed in a strikingly parallel and linear manner. Dashed lines indicate scaffold borders. The triangles indicate the axons in the grafts (c and f) or in the spinal cord adjacent to the injured cavity (i). The cell body-like structures are autofluorescent cells. Scale bars: A, D, and G, 300 μm; b, e, and h, 100 μm; c, f, and i, 25 μm. [Color figure can be viewed in the online issue, which is available at wileyonlinelibrary.com.]

staining (Fig. 3) demonstrated an extensive axonal growth into both the acellular muscle and the cell-seeded acellular muscle scaffolds 4 weeks postimplantation. The number of NF-positive nerve fibers was higher in the cell-seeded acellular muscle group than in the acellular muscle group (Fig. 4). However, the difference was not statistically significant. More strikingly, the majority of sprouting axons in both kinds of scaffold were distributed in a distinctly organized and linear fashion. In the injured group, no NF-positive nerve fibers were found in the lesional cavity.

To assess whether primary sensory axons and raphespinal axons grew in the scaffolds, CGRP and 5-HT immunohistochemistry were performed. The sensory axons that immunostained for CGRP were also found within the two kinds of the implant [Fig. 5(A,B)]. There was no statistical difference between the two treated groups [Fig. 5(C)]. However, for raphespinal axons, there was a significant difference between the two treated groups (Fig. 6). In the acellular muscle scaffold group, serotonin (5-HT)-positive axons stopped at the interface between the spinal cord and transplant. But in the cell-seeded acellular muscle group, they grew into the scaffold for a short distance.

The remyelination of the sprouting axons in the scaffolds was visualized by MBP-positive staining. The staining results

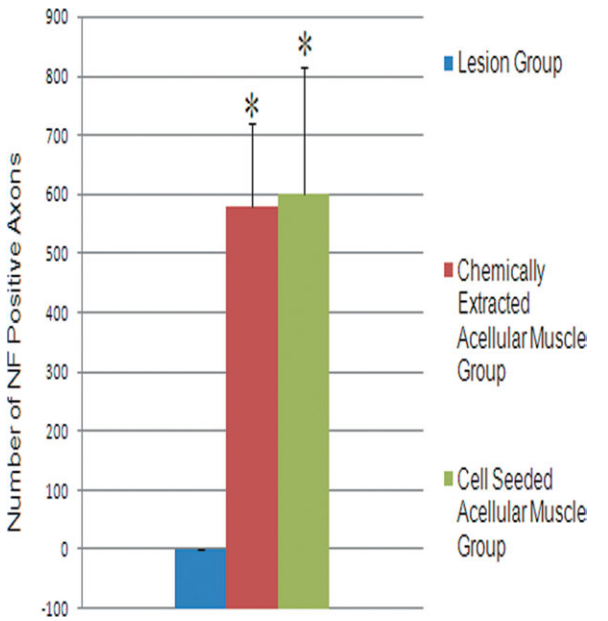

FIGURE 4. The number of NF positive nerve fibers in the scaffolds or at the injury site. *$p < 0.05$ versus the lesion control group. [Color figure can be viewed in the online issue, which is available at wileyonlinelibrary.com.]

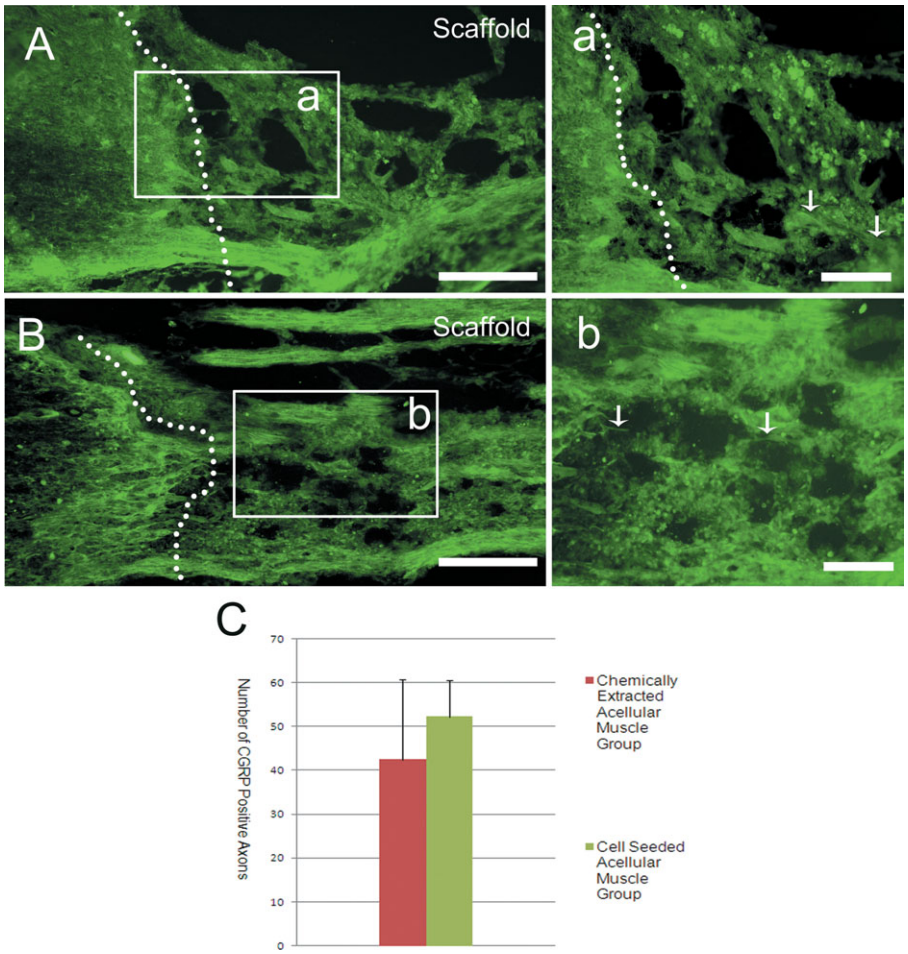

FIGURE 5. CGRP-immunolabeled sensory axons in the grafts 28 days after surgery. Coronal spinal cord sections show CGRP-positive sensory axons in the acellular muscle scaffold (A,a) and the acellular muscle scaffold with AECs injected during the implantation procedure (B,b). The broken lines mark the borders between the host spinal cords and grafts. The arrows point to the CGRP-positive axons in the grafts. C: Shows the numbers of CGRP positive axons within the two types of scaffolds. Scale bars: A and B, 250 μm; a and b, 100 μm. [Color figure can be viewed in the online issue, which is available at wileyonlinelibrary.com.]

showed that there were only a few myelinated axons in the acellular muscle scaffolds [Fig. 7(A)]. In contrast, the number of the myelinated axons in cell-seeded acellular muscle scaffolds increased dramatically [Fig. 7(B)]. The difference between the two groups was statistically significant [Fig. 7(C)].

Astrocytic response

The glial scar formation was evaluated by the GFAP staining of astrocytes. Immunofluorescence staining showed that reactive astrocytes were present in all subjects at the host/lesion interface (Fig. 8). This GFAP reactivity at the host/lesion interface did not differ qualitatively between the groups with and without scaffolds (Fig. 9). In the AECs-acellular muscle treated group, some astrocytes penetrated into the scaffold in a linear arrangement, parallel with the long axis of the scaffold (Fig. 8).

Functional recovery

Before surgery, all the rats showed normal locomotor performance with BBB scores of 21. The right (affected side) hind limb of the rats were completely paralyzed following T10 spinal cord hemisection. While SCI control rats had no

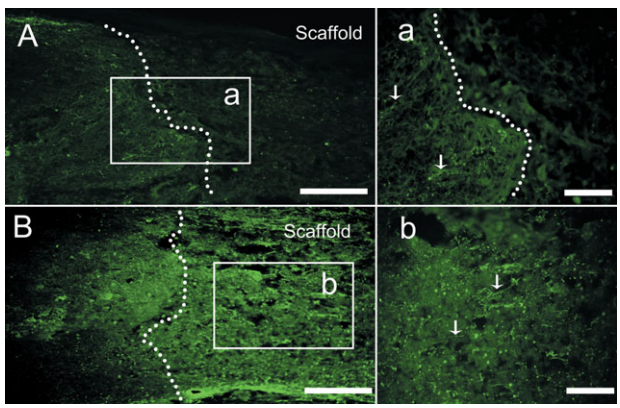

FIGURE 6. Coronal spinal cord sections showing raphespinal axons immunostained for serotonin (5-HT) at 4 weeks after SCI and following transplantation of the acellular muscle scaffold (A,a) and the acellular muscle scaffold seeded with AECs (B,b). The broken lines mark the borders between the host spinal cords and grafts. The arrows point to the serotonin-positive axons. Note that 5-HT axons penetrate into the AECs-acellular muscle scaffold. Scale bars: A and B, 250 μm; a and b, 100 μm. [Color figure can be viewed in the online issue, which is available at wileyonlinelibrary.com.]

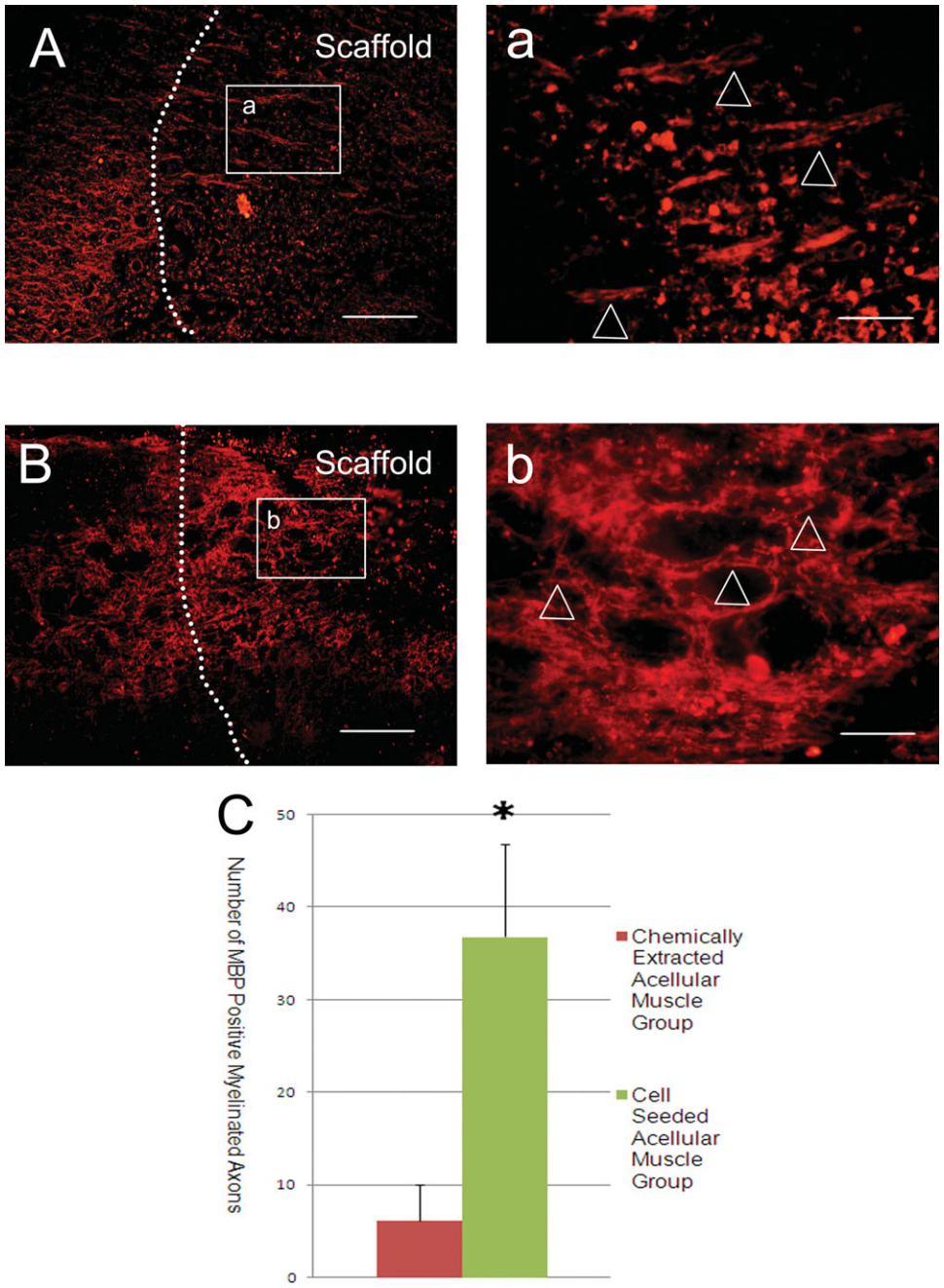

FIGURE 7. Sprouting myelinated nerve fibers in the chemically treated muscle (A,a) and the AECs-acellular muscle (B,b) 4 weeks after transplantation, MBP-positive staining. The broken lines mark the border between the spinal cords and grafts. The triangles point to the myelinated nerve fibers in the grafts. C: Shows the numbers of MBP positive myelinated axons within the two types of scaffolds. *Significant difference in the numbers of MBP positive axons ($p < 0.05$, *t*-test). The cell body-like structures are autofluorescent cells. Scale bars: A and B, 200 μm; a and b, 50 μm. [Color figure can be viewed in the online issue, which is available at wileyonlinelibrary.com.]

recovery, hind limb function showed small degrees of improvement in acellular muscle treated group, with the mean score of AECs-acellular muscle treated group being significantly higher than those of other groups (Fig. 10).

Electrophysiology

To further assess functional status of the severed spinal cord following implantation treatment, the CMEP and CSEP were measured. The data demonstrated that control rats with spinal cord hemitransection alone showed negligible signal level of both CMEPs and CSEPs (Fig. 11). Their latencies were prolonged and amplitudes were significantly lower compare with the normal control group (Tables I and II). But in the acellular muscle scaffold group, there were discernible recoveries in both the CMEP and CSEP compared with the SCI control group. Intriguingly, the AECs-acellular muscle treated group exhibited the highest degree of recovery in both latencies and amplitudes of the CMEP and CSEP.

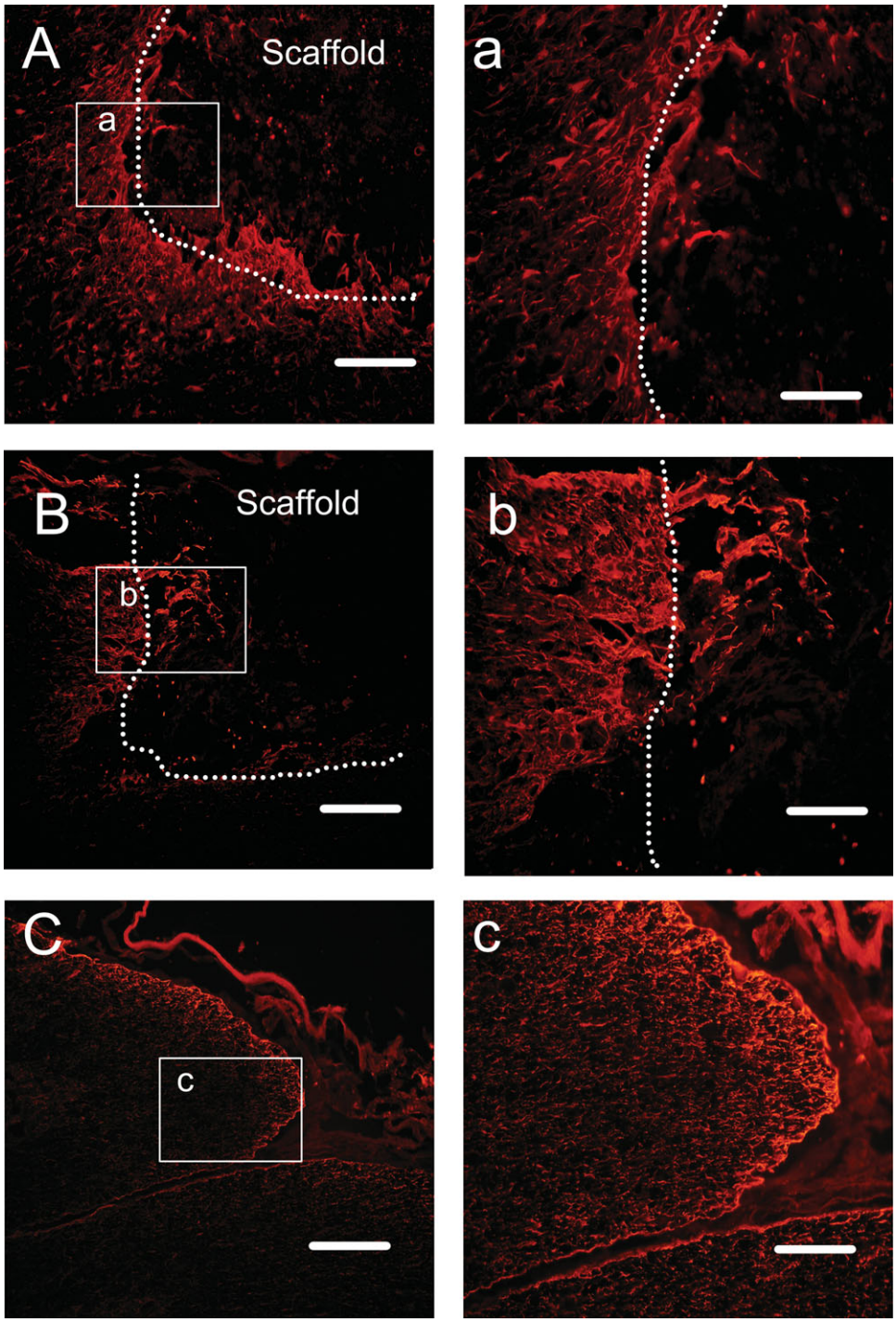

FIGURE 8. GFAP-positive astrocyte responses in each group. A and a: GFAP-positive cells in the chemically extracted acellular muscle treated group. B and b: GFAP-positive cells in the AECs-acellular muscle treated group. C and c: GFAP-positive cells in the lesion control group. The broken lines mark the border between the spinal cords and grafts. Scale bars: A, B, and C, 200 μm; a, b, and c, 50 μm. [Color figure can be viewed in the online issue, which is available at wileyonlinelibrary.com.]

DISCUSSION

In this study, we found that chemically extracted acellular muscle scaffolds seeded with AECs promoted axonal growth in a distinctly organized and linear fashion. The addition of AECs also promoted the remyelination of nerve fibers, improved relays of CMEP and CSEP, and stimulated regeneration of 5-HT nerve fibers. To our knowledge, these characteristics of AECs have not been tested before and suggest new possibilities for their use in the treatment of SCI.

Cell transplantation is an important tool that can provide neurotrophic factors for stimulating the intrinsic growth potential of injured neurons and/or to replace

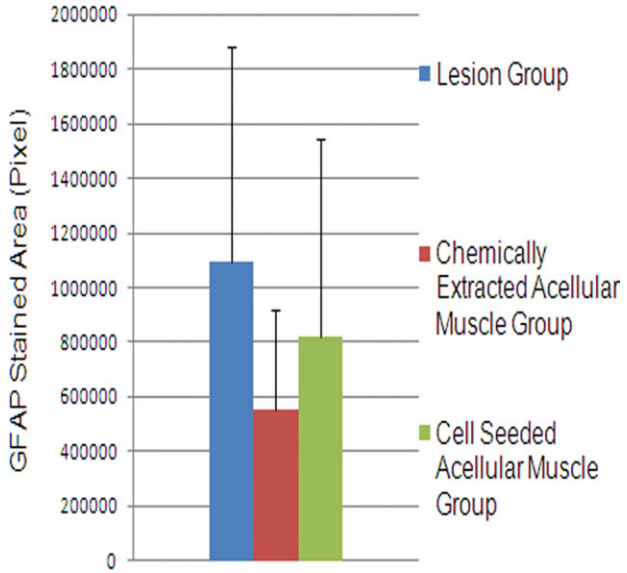

FIGURE 9. A comparison of GFAP-positive area between each group (n = 6). There is no statistically significant difference in the GFAP-positive area between the groups. [Color figure can be viewed in the online issue, which is available at wileyonlinelibrary.com.]

damaged or dead neurons after SCI. Previous studies have shown that grafting rat fetal spinal cord stem cells or progenitor cells into rats after SCI leads to improved anatomic growth/plasticity and functional recovery.[31] However, wider clinic use of fetal tissue comes against the double problem of obtaining a large enough quantity of the donor tissues and also of the ethical controversy surrounding the use of human fetal tissues. The solution to overcome such practical and ethical issues may lie in finding other tissue or cells to replace the fetal tissue. AECs express surface markers normally present on embryonic stem and germ cells.[22,32] In addition, AECs express the pluripotent stem cell-specific transcription factors octamer-binding protein 4 and nanog,[22] two genes known to be required for self-renewal and pluripotency. Correspondingly, the AECs can differentiate into all three germ layers—endoderm (liver, pancreas), mesoderm (cardiomyocytes), and ectoderm (neural cells) *in vitro*.[22,33,34] In our opinion, the AEC is one of the most promising cell candidates for stem cell-based therapy in the treatment of SCI.

In this investigation, we limited our focus to the therapeutic properties of AECs on SCI. Compared with the acellular muscle group, cotransplantation of AECs and acellular muscle better restored the function observed both physically and electrophysiologically in the hind limbs of treated SCI rats and promoted the sprouting of 5-HT axons and remyelination of sprouting axons. These data suggest that AECs can promote axonal remyelination, the sprouting of 5-HT axons, and functional recovery of SCI rats. This is in agreement with the previous reports, which have shown the capacity of AECs to promote the functional recovery of SCI in monkeys.[17] Our previous data[35] have also shown that AECs can promote the sprouting of NF-positive and CGRP-positive axons. All these characteristics demonstrate that AECs have high curative potential for the treatment of SCI.

The results of this study demonstrate that both acellular and cell-seeded scaffolds can promote the sprouting of NF-positive and CGRP-positive axons. There was no statistically significant difference between these two treated groups with regard to these axon numbers. In addition, 5-HT axons penetrated only a short distance into the AEC-scaffold transplant. Because there was only a small level of functional recovery in the acellular muscle group, the axonal sprouting seems not to be the main reason for the better functional recovery and the improved axonal conduction (CMEP and CSEP) in the AEC-acellular muscle treated group. In contrast, the number of remyelinated axons in AEC-acellular muscle treated group was significantly bigger than that of the acellular muscle group. Previous reports have shown that demyelination contributes to the dysfunction after traumatic SCI [36] and that remyelination of the denuded axons can improve the axonal conduction and facilitate functional recovery after SCI.[37] Similar to these reports, the remyelination promoted by the addition of AECs may play critical roles for the functional recovery and the enhanced axonal conduction in the AEC-acellular muscle treated group.

In the internal part of the AEC-acellular muscle grafts, we did not find neurons. This indicated that AECs did not differentiate into neural lineage cells. Thus, it was less possible that the AECs make the myelin sheath within the scaffolds. Our previous study has shown that the rat AECs could secrete NT-3 and BDNF.[25] It has been shown that NT-3 and BDNF could induce oligodendrocyte proliferation and myelination of regenerating axons after SCI.[38] Thus, the neurotrophic function of the rat AECs seemed to be the main reason for the remyelination in the AEC-acellular muscle treated group.

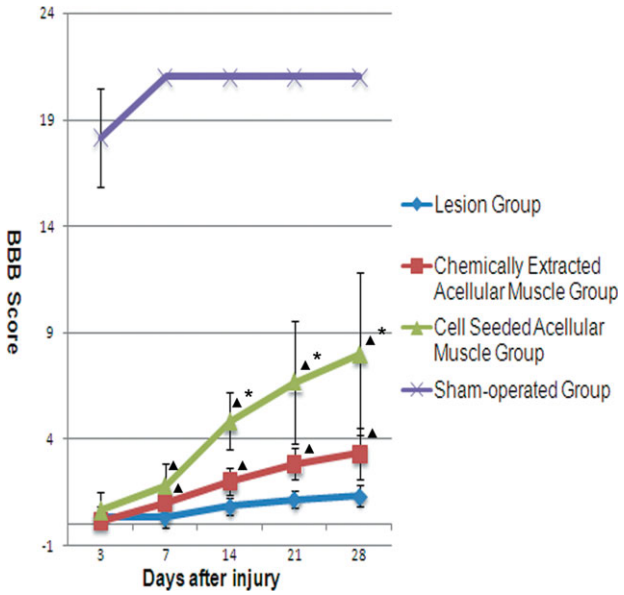

FIGURE 10. Comparison of BBB score of the affected side hind limb locomotor function in spinal cord hemisected rats of different study groups. ▲$p < 0.05$ versus the lesion control group. *$p < 0.05$ versus the chemically extracted acellular muscle treated group. [Color figure can be viewed in the online issue, which is available at wileyonlinelibrary.com.]

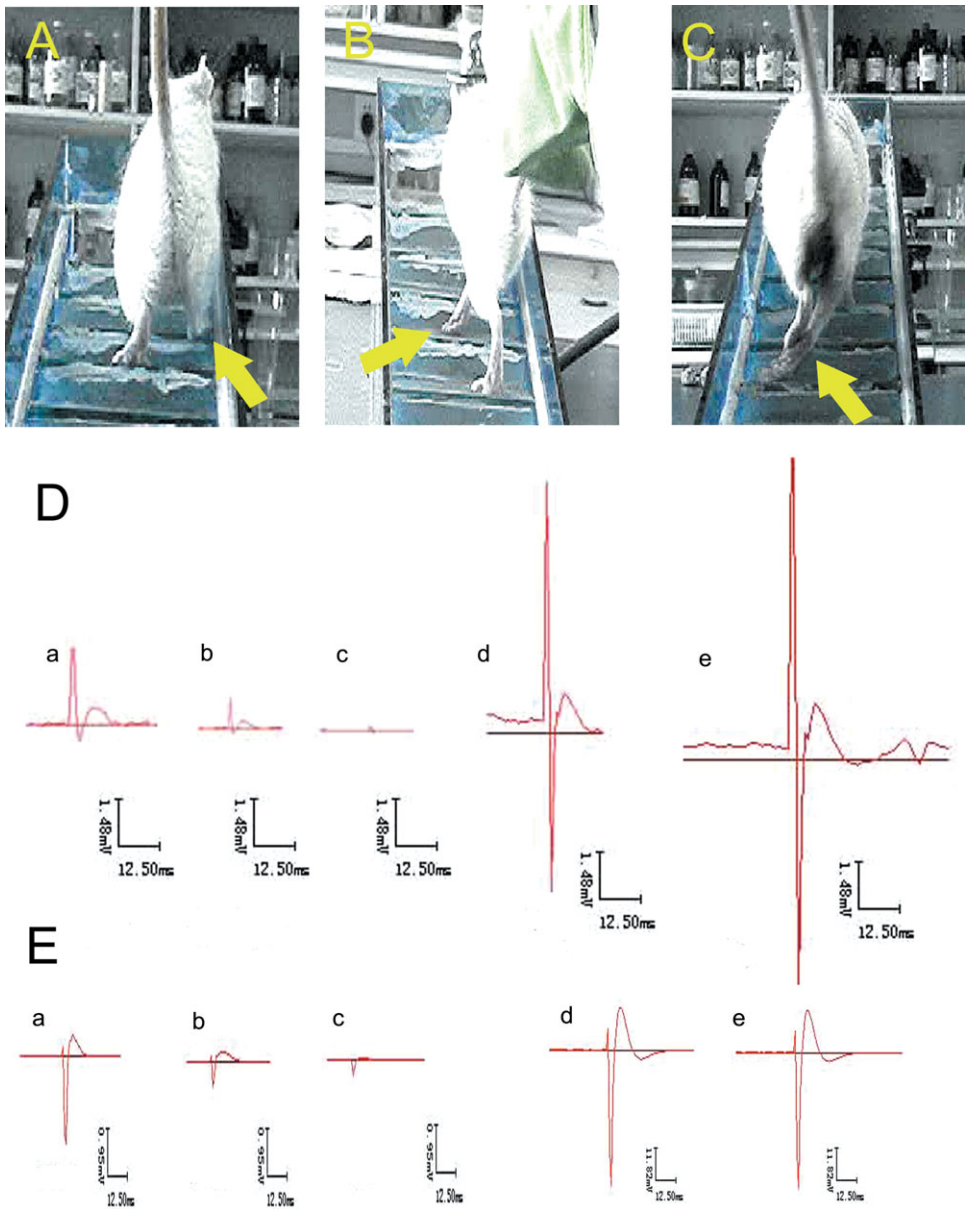

FIGURE 11. Analyses of behavioral and electrophysiological results. Upper panel: a representative image of the hind limbs of a SCI rat transplanted with the AECs-acellular muscle. Note that affected side hind limb (arrow) shows the weight-supported plantar step (A). The SCI rat treated only by acellular muscle shows the extensive movement of hip joint but no weight support step (arrow) (B). By contrast, the affected side hind limb of a representative control SCI rat remain behind (arrow) (C). Middle and lower panels: comparison of the average amplitude of CMEP (D) and CSEP (E) recorded in (a) the AECs-acellular muscle group, (b) acellular muscle alone, (c) SCI controls (note: negligible levels of signal), and (d) sham-operated controls or (e) normal rat controls. There is a discernible difference between the SCI control outcomes and that of the treated groups (a,b). The amplitude of CMEP and CSMP recovered best in the AECs-acellular muscle treated rats. [Color figure can be viewed in the online issue, which is available at wileyonlinelibrary.com.]

SCI usually induces significant secondary neuronal degeneration, and the chronic phase is characterized by the development of cysts and formation of glial scar. These structures can inhibit axonal regeneration, which cannot be solved by cell transplantation alone. There are also some major disadvantages for the implantation or injection of cells alone. One is the limited cell survival after the procedure, as implanted cells tend to desert the injury site.[39] Another problem for the transplantation of cells alone is their lack of 3D organization, typically resulting in random directions of axonal growth in the lesion. As a result, it is difficult for regenerating axons to be recruited for bridging beyond the lesion.[40] It may be possible that all these challenges can be solved by combining cell implants with the appropriate scaffold.

Chemically extracted acellular muscle provides a useful scaffold to combine with cell implants. Our recent study[14] showed that this scaffold has multiple characteristics

suitable for the treatment of spinal cord injuries. The acellular muscle can fill and bridge the cavity after SCI. It has good biocompatibility and integrates well with the host spinal cord. More importantly, this scaffold can promote axonal growth in a distinctly organized and linear fashion. In this study, we found that the acellular muscle can promote the growth of CGRP-positive axons. In the AEC-acellular muscle treated group, the muscle scaffold can also guide the sprouting axons in a controlled direction, indicating that the acellular muscle can solve the problem of lacking 3D organization for cell implants. In addition, the data showed that there were still a large number of Hoechst 33342-labeled AECs in the scaffolds 4 weeks after transplantation. Our previous results showed that only few Hoechst 33342-labeled AECs remained 2 weeks after cotransplantation into spinal cord with gelatin sponge.[35] This suggests the acellular muscle can prevent the AECs from leaving the injury site. There are other properties making the acellular muscle attractive for the treatment of SCIs. For example, acellular muscle has very low immunogenicity, potentially allowing allografting or perhaps even xenografting.[41,42] In fact, the evidence that the freeze-treated muscle or fresh muscle have been tested in clinical practice for the repair of damaged nerves[43] suggests that chemically extracted acellular muscle may be safe for clinical application.

There still are some potential technical issues in our experimental approach. It has been difficult for us to determine if the sprouting axons can migrate out from the scaffolds and into the distal stumps of the injured spinal cords. To improve this, completely transected spinal cord injured model and neuronal tract tracing techniques may need to be tested. The use of Hoechst dye to prelabel the nuclei of donor cells has the possibility that host uptake of this nuclear dye may occur. To prevent such potential contamination, we carefully washed the labeled cells. In addition, with the our previous finding[35] that only few Hoechst 33342-labeled cells remained 2 weeks after cotransplantation with gelatin sponges, we think that, to some extent, the Hoechst 33342-labeled results can reflect the survival of amnion epithelial cells in the acellular muscle scaffolds.

TABLE I. Comparison of the Amplitude and Latency of CMEP Between Uninjured Normal Rats and Spinal Cord Hemitransected Rats With Different Treatments ($n = 6$, $\bar{x} \pm s$)

Groups	Amplitude (mV)	Latency (mS)
Lesion group	0.24 ± 0.08	4.5 ± 0.53
Chemically extracted acellular muscle group	1.59 ± 0.09[a]	3.68 ± 0.12[a]
Cell-seeded acellular muscle group	2.84 ± 0.18[b]	2.9 ± 0.37[b]
Sham-operated group	21.6 ± 4.9	2.01 ± 0.02
Normal control group	23.3 ± 4.6	2.02 ± 0.02

One-way ANOVA followed by *t*-test:
[a] $p < 0.05$, versus lesion group.
[b] $p < 0.05$, versus lesion group and chemically extracted acellular muscle group.

TABLE II. Comparison of the Amplitude and Latency of CSEP Between Uninjured Normal Rats and Spinal Cord Hemitransected Rats With Different Treatments ($n = 6$, $\bar{x} \pm s$)

Groups	Amplitude (mV)	Latency (mS)
Lesion group	0.32 ± 0.16	4.05 ± 0.16
Chemically extracted acellular muscle group	0.8 ± 0.14[a]	3.64 ± 0.13[a]
Cell-seeded acellular muscle group	2.2 ± 0.12[b]	2.92 ± 0.1[b]
Sham-operated group	53.6 ± 13.3	2.06 ± 0.02
Normal control group	65.2 ± 12.2	2.05 ± 0.02

One-way ANOVA followed by *t*-test.
[a] $p < 0.05$, versus lesion group.
[b] $p < 0.05$, versus lesion group and chemically extracted acellular muscle group.

CONCLUSIONS

Taking all these observations together, chemically extracted acellular muscle seeded with AECs promoted axonal sprouting, remyelination, and functional recovery after SCI. This suggests the possibility that such an approach may become a valuable therapeutic strategy for spinal cord repair.

REFERENCES

1. Benowitz LI, Yin Y. Combinatorial treatments for promoting axon regeneration in the CNS: strategies for overcoming inhibitory signals and activating neurons' intrinsic growth state. Dev Neurobiol 2007;67:1148–1165.
2. Blesch A, Tuszynski MH. Spinal cord injury: plasticity, regeneration and the challenge of translational drug development. Trends Neurosci 2009;32:41–47.
3. King VR, Henseler M, Brown RA, Priestley JV. Mats made from fibronectin support oriented growth of axons in the damaged spinal cord of the adult rat. Exp Neurol 2003;182:383–398.
4. Yoshii S, Oka M, Shima M, Akagi M, Taniguchi A. Bridging a spinal cord defect using collagen filament. Spine (Phila Pa 1976) 2003;28:2346–2351.
5. Blesch A, Tuszynski MH. Cellular GDNF delivery promotes growth of motor and dorsal column sensory axons after partial and complete spinal cord transections and induces remyelination. J Comp Neurol 2003;467:403–417.
6. Bradbury EJ, Khemani S, Von R, King, Priestley JV, McMahon SB. NT-3 promotes growth of lesioned adult rat sensory axons ascending in the dorsal columns of the spinal cord. Eur J Neurosci 1999;11:3873–3883.
7. Schnell L, Schwab ME. Axonal regeneration in the rat spinal cord produced by an antibody against myelin-associated neurite growth inhibitors. Nature 1990;343:269–272.
8. Bradbury EJ, Moon LD, Popat RJ, King VR, Bennett GS, Patel PN, Fawcett JW, McMahon SB. Chondroitinase ABC promotes functional recovery after spinal cord injury. Nature 2002;416:636–640.
9. Nomura H, Tator CH, Shoichet MS. Bioengineered strategies for spinal cord repair. J Neurotrauma 2006;23:496–507.
10. Subramanian A, Krishnan UM, Sethuraman S. Development of biomaterial scaffold for nerve tissue engineering: Biomaterial mediated neural regeneration. J Biomed Sci 2009;16:108.
11. Willerth SM, Sakiyama-Elbert SE. Approaches to neural tissue engineering using scaffolds for drug delivery. Adv Drug Deliv Rev 2007;59:325–338.
12. Stokols S, Tuszynski MH. Freeze-dried agarose scaffolds with uniaxial channels stimulate and guide linear axonal growth following spinal cord injury. Biomaterials 2006;27:443–451.
13. Madigan NN, McMahon S, O'Brien T, Yaszemski MJ, Windebank AJ. Current tissue engineering and novel therapeutic approaches

to axonal regeneration following spinal cord injury using polymer scaffolds. Respir Physiol Neurobiol 2009;169:183–199.
14. Zhang X-Y, Xue H, Liu J-M, Chen D. Chemically extracted acellular muscle: a new potential scaffold for spinal cord injury repair. J Biomed Mater Res A 2012;100A:578–587.
15. Jones LL, Oudega M, Bunge MB, Tuszynski MH. Neurotrophic factors, cellular bridges and gene therapy for spinal cord injury. J Physiol 2001;533(Pt 1):83–89.
16. Plant GW, Christensen CL, Oudega M, Bunge MB. Delayed transplantation of olfactory ensheathing glia promotes sparing/regeneration of supraspinal axons in the contused adult rat spinal cord. J Neurotrauma 2003;20:1–16.
17. Sankar V, Muthusamy R. Role of human amniotic epithelial cell transplantation in spinal cord injury repair research. Neuroscience 2003;118:11–17.
18. Diaz-Prado S, Muinos-Lopez E, Hermida-Gomez T, Cicione C, Rendal-Vazquez ME, Fuentes-Boquete I, de Toro FJ, Blanco FJ. Human amniotic membrane as an alternative source of stem cells for regenerative medicine. Differentiation 2011;81:162–171.
19. Sakuragawa N, Tohyama J, Yamamoto H. Immunostaining of human amniotic epithelial cells: possible use as a transgene carrier in gene therapy for inborn errors of metabolism. Cell Transplant 1995;4:343–346.
20. Akle CA, Adinolfi M, Welsh KI, Leibowitz S, McColl I. Immunogenicity of human amniotic epithelial cells after transplantation into volunteers. Lancet 1981;2:1003–1005.
21. Toda A, Okabe M, Yoshida T, Nikaido T. The potential of amniotic membrane/amnion-derived cells for regeneration of various tissues. J Pharmacol Sci 2007;105:215–228.
22. Miki T, Lehmann T, Cai H, Stolz DB, Strom SC. Stem cell characteristics of amniotic epithelial cells. Stem Cells 2005;23:1549–1559.
23. Chen Z, Lu XC, Shear DA, Dave JR, Davis AR, Evangelista CA, Duffy D, Tortella FC. Synergism of human amnion-derived multipotent progenitor (AMP) cells and a collagen scaffold in promoting brain wound recovery: pre-clinical studies in an experimental model of penetrating ballistic-like brain injury. Brain Res 2011; 1368:71–81.
24. Uchida S, Inanaga Y, Kobayashi M, Hurukawa S, Araie M, Sakuragawa N. Neurotrophic function of conditioned medium from human amniotic epithelial cells. J Neurosci Res 2000;62:585–590.
25. Meng XT, Chen D, Dong ZY, Liu JM. Enhanced neural differentiation of neural stem cells and neurite growth by amniotic epithelial cell co-culture. Cell Biol Int 2007;31:691–698.
26. Mligiliche N, Kitada M, Ide C. Grafting of detergent-denatured skeletal muscles provides effective conduits for extension of regenerating axons in the rat sciatic nerve. Arch Histol Cytol 2001; 64:29–36.
27. Basso DM, Beattie MS, Bresnahan JC. A sensitive and reliable locomotor rating scale for open field testing in rats. J Neurotrauma 1995;12:1–21.
28. Taylor SJ, Rosenzweig ES, McDonald JW III, Sakiyama-Elbert SE. Delivery of neurotrophin-3 from fibrin enhances neuronal fiber sprouting after spinal cord injury. J Control Release 2006;113: 226–235.
29. Pan HC, Cheng FC, Lai SZ, Yang DY, Wang YC, Lee MS. Enhanced regeneration in spinal cord injury by concomitant treatment with granulocyte colony-stimulating factor and neuronal stem cells. J Clin Neurosci 2008;15:656–664.
30. Guo J, Su H, Zeng Y, Liang YX, Wong WM, Ellis-Behnke RG, So KF, Wu W. Reknitting the injured spinal cord by self-assembling peptide nanofiber scaffold. Nanomedicine 2007;3:311–321.
31. Nakamura M, Okano H, Toyama Y, Dai HN, Finn TP, Bregman BS. Transplantation of embryonic spinal cord-derived neurospheres support growth of supraspinal projections and functional recovery after spinal cord injury in the neonatal rat. J Neurosci Res 2005;81:457–468.
32. Miki T, Mitamura K, Ross MA, Stolz DB, Strom SC. Identification of stem cell marker-positive cells by immunofluorescence in term human amnion. J Reprod Immunol 2007;75:91–96.
33. Marongiu F, Gramignoli R, Dorko K, Miki T, Ranade AR, Paola Serra M, Doratiotto S, Sini M, Sharma S, Mitamura K, Sellaro TL, Tahan V, Skvorak KJ, Ellis EC, Badylak SF, Davila JC, Hines R, Laconi E, Strom SC. Hepatic differentiation of amniotic epithelial cells. Hepatology 2011;53:1719–1729.
34. Shinya M, Komuro H, Saihara R, Urita Y, Kaneko M, Liu Y. Neural differentiation potential of rat amniotic epithelial cells. Fetal Pediatr Pathol 2010;29:133–143.
35. Li C, Xue H, Liu J-M, Zhang X-Y, Song Y, Wang J-C. Promotional effects of amniotic epithelial cells on neural regeneration in spinal cord hemisection-injured rats. J Jilin Univ (Med Ed) 2011;37: 202–206.
36. Cao Q, Zhang YP, Iannotti C, DeVries WH, Xu XM, Shields CB, Whittemore SR. Functional and electrophysiological changes after graded traumatic spinal cord injury in adult rat. Exp Neurol 2005; 191(suppl 1):S3–S16.
37. McDonald JW, Liu XZ, Qu Y, Liu S, Mickey SK, Turetsky D, Gottlieb DI, Choi DW. Transplanted embryonic stem cells survive, differentiate and promote recovery in injured rat spinal cord. Nat Med 1999;5:1410–1412.
38. McTigue DM, Horner PJ, Stokes BT, Gage FH. Neurotrophin-3 and brain-derived neurotrophic factor induce oligodendrocyte proliferation and myelination of regenerating axons in the contused adult rat spinal cord. J Neurosci 1998;18:5354–5365.
39. Rochkind S, Shahar A, Fliss D, El-Ani D, Astachov L, Hayon T, Alon M, Zamostiano R, Ayalon O, Biton IE, Cohen Y, Halperin R, Schneider D, Oron A, Nevo Z. Development of a tissue-engineered composite implant for treating traumatic paraplegia in rats. Eur Spine J 2006;15:234–245.
40. Gros T, Sakamoto JS, Blesch A, Havton LA, Tuszynski MH. Regeneration of long-tract axons through sites of spinal cord injury using templated agarose scaffolds. Biomaterials 2010;31:6719–6729.
41. Kvist M, Sondell M, Kanje M, Dahlin LB. Regeneration in, and properties of, extracted peripheral nerve allografts and xenografts. J Plast Surg Hand Surg 2011;45:122–128.
42. Fansa H, Schneider W, Wolf G, Keilhoff G. Host responses after acellular muscle basal lamina allografting used as a matrix for tissue engineered nerve grafts1. Transplantation 2002;74: 381–387.
43. Houstava L, Dubovy P, Haninec P, Grim M. An alternative preparation of the acellular muscle graft for reconstruction of the injured nerve—morphological and morphometric analysis. Ann Anat 1999;181:275–281.